





In the format provided by the authors and unedited.

# Age-dependent effects in the transmission and control of COVID-19 epidemics

Nicholas G. Davies <sup>1</sup>✉, Petra Klepac<sup>1,2</sup>, Yang Liu<sup>1,2</sup>, Kiesha Prem <sup>1</sup>, Mark Jit <sup>1</sup>, CMMID COVID-19 working group and Rosalind M. Eggo <sup>1</sup>✉

---

<sup>1</sup>Department of Infectious Disease Epidemiology, London School of Hygiene & Tropical Medicine, London, UK. <sup>2</sup>These authors contributed equally: Petra Klepac, Yang Liu. ✉e-mail: [nicholas.davies@lshtm.ac.uk](mailto:nicholas.davies@lshtm.ac.uk); [r.eggo@lshtm.ac.uk](mailto:r.eggo@lshtm.ac.uk)

## Age-dependent effects in the transmission and control of COVID-19 epidemics

Authors: Nicholas G. Davies<sup>1\*</sup>, Petra Klepac<sup>1^</sup>, Yang Liu<sup>1^</sup>, Kiesha Prem<sup>1</sup>, Mark Jit<sup>1</sup>, CMMID COVID-19 working group, Rosalind M Eggo<sup>1\*</sup>

The CMMID COVID-19 working group<sup>1</sup> is: Carl A B Pearson, Billy J Quilty, Adam J Kucharski, Hamish Gibbs, Samuel Clifford, Amy Gimma, Kevin van Zandvoort, James D Munday, Charlie Diamond, W John Edmunds, Rein MGJ Houben, Joel Hellewell, Timothy W Russell, Sam Abbott, Sebastian Funk, Nikos I Bosse, Fiona Sun, Stefan Flasche, Alicia Rosello & Christopher I Jarvis. Order of working group determined at random.

<sup>1</sup> Department of Infectious Disease Epidemiology, London School of Hygiene & Tropical Medicine, Keppel Street, WC1E 7HT

<sup>^</sup> these authors contributed equally

\* correspondence to Rosalind M Eggo [r.eggo@lshtm.ac.uk](mailto:r.eggo@lshtm.ac.uk) or Nicholas G Davies [nicholas.davies@lshtm.ac.uk](mailto:nicholas.davies@lshtm.ac.uk)

Parameter	Description	Applies in fits	Value	Reference
$d_E$	Incubation period (E to I <sub>P</sub> and E to I <sub>S</sub> ; days)	All	$\sim \text{gamma}(\mu = 3.0, k = 4)$	Derived from refs. 1,2
$d_P$	Duration of preclinical infectiousness (days)	All	$\sim \text{gamma}(\mu = 2.1, k = 4)$	Derived from ref. 2
$d_C$	Duration of clinical infectiousness (I <sub>C</sub> to R; days)	All	$\sim \text{gamma}(\mu = 2.9, k = 4)$	Ref. 3
$d_S$	Duration of subclinical infectiousness (days)	All	$\sim \text{gamma}(\mu = 5, k = 4)$	Assumed
$u_i$	Susceptibility for age group $i$	Varies by age in Wuhan hypothesis 2, otherwise all ages equal	Estimated	
$y_i$	Probability of clinical infection for age group $i$	Varies by age in Wuhan hypothesis 3, otherwise all ages equal	Either fixed (50%) or estimated	Ref. 4
$f$	Relative infectiousness of subclinical cases	All	50% (0% and 100% in sensitivity analysis)	Assumed
$c_{ij}$	Number of age- $j$ individuals contacted by an age- $i$ individual per day	All	Country-specific contact matrix.	China <sup>5</sup> ; UK <sup>6</sup> ; Zimbabwe <sup>7</sup>
$N_i$	Number of age- $i$ individuals	All	Demographic data	Ref. 8
$\Delta t$	Time step for discrete-time simulation	All	0.25 days	
$A_{min}, A_{max}$	Age range of seed cases	Wuhan	Estimated	
$t_{seed}$	Day upon which seeding of infections starts	All	Estimated	
$q_H$	Relative change in non-school contacts during lunar new year holidays	Wuhan	Estimated	
$q_L$	Relative change in non-school contacts following large-scale restrictions	Wuhan, South Korea, Shanghai, Beijing, Italy	Estimated	
$t_L$	Day upon which large-scale restrictions start	Wuhan, South Korea, Shanghai, Beijing, Italy	Fixed to January 23 for Wuhan; estimated for other settings	

**Supplementary Table 1.** Model parameters.

Parameter	Description	Prior
$u_i$	Susceptibility to infection upon contact with an infectious person	<p>Non-age-varying: <math>u_i \sim normal(\mu = 0.1, \sigma = 0.025, min = 0)</math></p> <p>Age-varying: young, middle, and old age fit as  <math>a_y \sim normal(\mu = 15, \sigma = 15, min = 0, max = 30)</math>  <math>a_m \sim normal(\mu = 45, \sigma = 15, min = 30, max = 60)</math>  <math>a_o \sim normal(\mu = 75, \sigma = 15, min = 60, max = 90)</math></p> <p>Susceptibility for young, middle, and old age fit as  <math>u_y \sim normal(\mu = 0.1, \sigma = 0.025, min = 0)</math>  <math>u_m \sim normal(\mu = 0.1, \sigma = 0.025, min = 0)</math>  <math>u_o \sim normal(\mu = 0.1, \sigma = 0.025, min = 0)</math></p> <p>Then  <math>u_i = coss(i a_y, b_y, a_m, b_m, a_o, b_o)</math> (see final row)</p>
$y_i$	Clinical fraction on infection	<p>Non-age-varying: <math>y_i = 0.5</math></p> <p>Age-varying: young, middle, and old age fit as  <math>a_y \sim normal(\mu = 15, \sigma = 15, min = 0, max = 30)</math>  <math>a_m \sim normal(\mu = 45, \sigma = 15, min = 30, max = 60)</math>  <math>a_o \sim normal(\mu = 75, \sigma = 15, min = 60, max = 90)</math></p> <p>Susceptibility for young, middle, and old age fit as  <math>y_y \sim normal(\mu = 0.5, \sigma = 0.1, min = 0, max = 0.5)</math>  <math>y_m = 0.5</math>  <math>y_o \sim normal(\mu = 0.5, \sigma = 0.1, min = 0.5, max = 1)</math></p> <p>Then  <math>y_i = coss(i a_y, y_y, a_m, y_m, a_o, y_o)</math> (see below)</p>
$t_{seed}$	Timing of introduction of cases	$t_{seed} \sim normal(\mu = 15, \sigma = 30, min = 0, max = 30)$
$q_H$	Multiplicative factor for transmission during holiday period	$q_H \sim beta(\alpha = 2, \beta = 2)$ scaled to 0 – 2
$q_L$	Multiplicative factor for transmission during large-scale restrictions	$q_L \sim beta(\alpha = 2, \beta = 2)$
$A_{min}, A_{max}$	Age bounds for introduced cases	$A \sim normal(\mu = 60, \sigma = 20, min = 40, max = 80)$ $A_{range} \sim beta(\alpha = 2, \beta = 2)$ scaled to 0 – 10 $A_{min} = A - A_{range}$ $A_{max} = A + A_{range}$
$coss(a x_1, y_1, x_2, y_2, x_3, y_3)$	Cosine-smoothing function	For a given age $a$ (the midpoint age of age group $i$ ) the function evaluates to $y_1$ for $a \leq x_1$ , to $y_2$ for $a = x_2$ , and to $y_3$ for $a \geq x_3$ . Values of $a$ between $x_1$ and $x_2$ are interpolated between $y_1$ and $y_2$ , and values of $a$ between $x_2$ and $x_3$ are interpolated between $y_2$ and $y_3$ , where the interpolation takes the shape of a cosine curve between $-\pi$ and $\pi$ .

Supplementary Table 2. Details of model fitting.

Location	Mixing matrix details
Wuhan City, China	We used mixing matrices measured in Shanghai in 2017/2018 <sup>5</sup> , adapted to the demographics of Wuhan prefecture. This implicitly assumes that Shanghai mixing patterns are representative of large cities in China.
Regions of China: Anhui, Guangdong, Guangxi, Hubei, Hunan, Jiangsu, Jiangxi, Jilin Shaanxi, Shandong, Sichuan, Tianjin, Zhejiang provinces; Beijing, Shanghai.	We used mixing matrices measured in Shanghai in 2017/2018 <sup>5</sup> , adapted to the demographics of each province / city.
Regions of Italy: Lombardia, Piemonte, Trento Veneto, Friuli Venezia Giulia, Liguria, Emilia-Romagna, Toscana, Marche, Lazio, Campania, Puglia regions; Milan.	We used mixing matrices measured in Italy in 2005/2006 <sup>6</sup> , adapted to the demographics of each region / city. This assumes that these contact patterns will still be representative of contact patterns in 2020.
Ontario, Canada	We used synthetic contact matrices, generated based on demographic information about the country <sup>9</sup> .
Japan	We used synthetic contact matrices, generated based on demographic information about the country <sup>9</sup> .
Singapore	We used synthetic contact matrices based on demographic information about the country <sup>9</sup> .
South Korea	We used synthetic contact matrices based on demographic information about the country <sup>9</sup> .
Birmingham, UK	We used mixing matrices measured in the UK in 2005/2006 <sup>6</sup> , adapted to the demographics of Birmingham. This assumes that these contact patterns will still be representative of contact patterns in 2020.
Bulawayo, Zimbabwe	We used mixing matrices measured in Manicaland, Zimbabwe in 2013 <sup>7</sup> , adapted to the demographics of Bulawayo. This implicitly assumes that Manicaland mixing patterns are representative of Bulawayo.
146 capital cities	We used synthetic contact matrices, generated based on demographic information about each country <sup>9</sup> .

**Supplementary Table 3.** Details on mixing matrices used in the study.

Wuhan: Model 1		
age_y	6	(4.2-7.2)
age_m	55	(46-60)
age_o	64	(60-68)
susc_y	0.003	(0.00014-0.0076)
susc_m	0.044	(0.032-0.054)
susc_o	0.084	(0.079-0.09)
seed_start	19	(16-22)
seed_age	61	(42-79)
seed_age_range	4.9	(1.5-8.9)
qH	1.4	(1.3-1.5)
qL	0.41	(0.3-0.56)
Wuhan: Model 2		
age_y	19	(14-29)
age_m	50	(40-60)
age_o	68	(60-79)
susc	0.055	(0.052-0.059)
symp_y	0.037	(0.0051-0.062)
symp_m	0.3	(0.19-0.42)
symp_o	0.65	(0.52-0.77)
seed_start	16	(14-20)
seed_age	46	(30-67)
seed_age_range	1.3	(0.5-1.9)
qH	1.3	(1.2-1.4)
qL	0.43	(0.31-0.56)
Wuhan: Model 3		
susc	0.046	(0.045-0.048)
seed_start	20	(17-21)
seed_age	64	(37-80)
seed_age_range	4.2	(0.93-8.7)
qH	1.4	(1.3-1.5)
qL	0.33	(0.21-0.42)
Beijing, Shanghai		
susc	0.074	(0.055-0.1)
B_seed_t0	20	(15-25)
S_seed_t0	21	(16-26)
seed_d	3.8	(1.4-6.2)
lockdown_t	54	(53-56)
qH	1.2	(0.71-1.7)
qL	0.16	(0.11-0.22)
	0.074	(0.055-0.1)
South Korea		
susc	0.099	(0.089-0.11)
seed_t0	8.3	(5-12)
seed_d	3.3	(0.79-6.2)
lockdown_t	53	(52-54)
qL	0.047	(0.0041-0.095)
Lombardy		
susc	0.084	(0.075-0.096)
conf_mean	7.6	(2.7-13)
conf_shape	11	(3.7-20)
onset_known	0.36	(0.061-0.62)
seed_t0	15	(11-20)
seed_d	3.6	(0.83-6.3)
lockdown_t	50	(47-54)
qL	0.48	(0.28-0.72)

**Supplementary Table 4.** Posterior means and 95% HDIs from fitting the dynamic transmission model (Figs. 1 and 2, main text).

## Supplementary references

1. Lauer, S. A. et al. The Incubation Period of Coronavirus Disease 2019 (COVID-19) From Publicly Reported Confirmed Cases: Estimation and Application. *Ann. Intern. Med.* (2020) doi:10.7326/M20-0504.
2. Backer, J. A., Klinkenberg, D. & Wallinga, J. Incubation period of 2019 novel coronavirus (2019-nCoV) infections among travellers from Wuhan, China, 20–28 January 2020. *Eurosurveillance* 25, (2020).
3. Kucharski, A. J. et al. Early dynamics of transmission and control of COVID-19: a mathematical modelling study. *Lancet Infect. Dis.* S1473309920301444 (2020) doi:10.1016/S1473-3099(20)30144-4.
4. Nishiura, H. et al. The Rate of Underascertainment of Novel Coronavirus (2019-nCoV) Infection: Estimation Using Japanese Passengers Data on Evacuation Flights. *J. Clin. Med.* 9, 419 (2020).
5. Zhang, J. et al. Patterns of human social contact and contact with animals in Shanghai, China. *Sci. Rep.* 9, 1–11 (2019).
6. Mossong, J. et al. Social Contacts and Mixing Patterns Relevant to the Spread of Infectious Diseases. *PLOS Med.* 5, e74 (2008).
7. Melegaro, A. et al. Social Contact Structures and Time Use Patterns in the Manicaland Province of Zimbabwe. *PLOS ONE* 12, e0170459 (2017).
8. World Population Prospects - Population Division - United Nations. <https://population.un.org/wpp/>.
9. Prem, K., Cook, A. R. & Jit, M. Projecting social contact matrices in 152 countries using contact surveys and demographic data. *PLOS Comput. Biol.* 13, e1005697 (2017).